Workbench for 3D target detection and recognition from airborne motion stereo and ladar imagery

Simon Roy[a*], Stephen Se[b], Vinay Kotamraju[b], Jean Maheux[a], Christian Nadeau[b], Vincent Larochelle[a] and Jonathan Fournier[a]

[a]Defence Research and Development Canada, 2459 Pie-XI Blvd. North, Québec, QC, Canada
[b]MDA Systems Ltd., 13800 Commerce Parkway, Richmond, BC, Canada

ABSTRACT

3D imagery has a well-known potential for improving situational awareness and battlespace visualization by providing enhanced knowledge of uncooperative targets. This potential arises from the numerous advantages that 3D imagery has to offer over traditional 2D imagery, thereby increasing the accuracy of automatic target detection (ATD) and recognition (ATR). Despite advancements in both 3D sensing and 3D data exploitation, 3D imagery has yet to demonstrate a true operational gain, partly due to the processing burden of the massive dataloads generated by modern sensors. In this context, this paper describes the current status of a workbench designed for the study of 3D ATD/ATR. Among the project goals is the comparative assessment of algorithms and 3D sensing technologies given various scenarios. The workbench is comprised of three components: a database, a toolbox, and a simulation environment. The database stores, manages, and edits input data of various types such as point clouds, video, still imagery frames, CAD models and metadata. The toolbox features data processing modules, including range data manipulation, surface mesh generation, texture mapping, and a shape-from-motion module to extract a 3D target representation from video frames or from a sequence of still imagery. The simulation environment includes synthetic point cloud generation, 3D ATD/ATR algorithm prototyping environment and performance metrics for comparative assessment. In this paper, the workbench components are described and preliminary results are presented. Ladar, video and still imagery datasets collected during airborne trials are also detailed.

Keywords: 3D imagery, Ladar, Lidar, Motion stereo, Shape-from-motion, Automatic target detection, Automatic target recognition, ISR

1. INTRODUCTION

Automatic Target Detection (ATD) and Automatic Target Recognition (ATR) are essential for Intelligence, Surveillance, and Reconnaissance (ISR) missions. There are two fundamental challenges in ATD/ATR for ISR. The first is the massive dataloads generated by modern high-resolution sensors, which can quickly escalate to unmanageable proportions. Since effective tactical battlefield management depends on timely and trustworthy information, efficient and accurate algorithms are required to quickly extract analysis-ready information while sparing the end-user of the post-processing burden. The second challenge is Camouflage, Concealment, and Deception (CC&D). Uncooperative targets go to great extends to minimize the diffusion of information about themselves by hiding, camouflaging or deploying decoys. This further increases the complexity of ATD/ATR and motivates the need for robust techniques.

A promising approach to tackle these challenges is 3D imagery. It is widely acknowledged that 3D imagery offers many advantages over traditional 2D imagery,[1–3] implying new venues for ATR and a potential for increased accuracy. 3D imagery enhances the descriptiveness of target signatures, which can be extracted directly from widely available CAD models. Additionally, certain 3D sensing techniques such as ladar[4] provide foliage and camouflage penetration. This simplifies foreground and background clutter removal, facilitates target detection and segmentation, and yields higher recognition rates and lower false alarms rates. Moreover, 3D imagery enables recognition by parts,[5,6] which is highly appealing when considering articulate targets, improvised fighting vehicles and the countless possibilities of target configurations.

* Corresponding author: simon.roy@drdc-rddc.gc.ca, www.valcartier.drdc-rddc.gc.ca

1.1 Motivations and Outline

In this context, a workbench is currently being developed at MDA Systems Ltd. for DRDC Valcartier. The workbench will be the primary tool in a study of 3D ATD/ATR, which will focus on evaluating algorithms and 3D sensing technologies given various scenarios. This work aims at improving situational awareness and battlespace visualization by enabling airborne tactical ISR platforms to provide timely, relevant and accurate knowledge of uncooperative targets.

This paper will first describe the workbench and its capabilities. Two recent data collection trials will then be discussed. The first is a high-resolution vehicle scanning campaign to populate the model database. The second is an airborne field trial featuring scenarios for various levels of target cooperation. Preliminary results will then be presented, followed by a discussion of future work.

2. WORKBENCH DESCRIPTION

The DRDC workbench is comprised of three components: a database, a toolbox for data processing and 3D ATD/ATR simulation environments. Fig. 1 depicts the high-level process flow diagram of the system. The workbench supports various input data types, such as range data, image sequences, video, CAD models, Digital Terrain Models (DTMs), navigation data and sensor parameters.

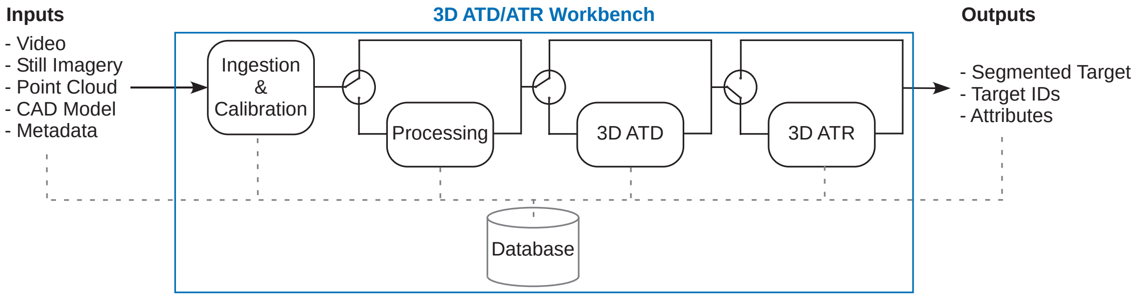

Figure 1. High-level process flow diagram of the 3D ATD/ATR workbench.

The input data is first converted to a native format and calibrated when required. The data may then be manipulated with tools from the Processing Module described in Section 3.2. The raw or processed data may be passed to the 3D ATD Module, and/or to the 3D ATR Module. This configuration allows the user to independently study either the ATD process or the ATR process, and also permits the study of full ATD/ATR pipelines.

The 3D ATD Module locates potential targets in the 3D representation of a scene. This module is designed to include algorithms for target detection, target classification and target segmentation. Generally, this process includes ground surface estimation and man-made object detection to significantly downsize the scene data. Suspected target areas are segmented into Volumes of Interest (VOIs) which may then be passed to the 3D ATR Module for further analysis. Hence, the 3D ATD Module does not require knowledge of the target objects.

The 3D ATR Module analyses VOIs either segmented by the ATD module or manually generated with tools from the Processing Module. This module is designed to include algorithms for signature extraction, signature matching and performance evaluation. Generally, ATR algorithms encode the shape of an object into a set of descriptive signatures. This simplifies and accelerates the matching process. An offline phase is required to extract signatures for each 3D model in a library. During the online phase, signatures are extracted from each VOI and signature matching identifies the most probable match between the VOI signature and the 3D models in the library.

The source datasets and 3D models are therefore maintained in a database, along with processed data at any point in the pipeline. Data may thus be easily retrieved for ATD/ATR testing and results may be compared for various algorithms, sensors and datasets.

2.1 Hardware

The workbench is a 3D data processing station based on high-performance off-the-shelf hardware components. Listed in Table 1, these components are selected according to requirements for a multi-core/multi-processor architecture. A large memory is required for providing high processing speed and a large disk space is necessary to support database requirements.

Table 1. Hardware components of the 3D ATD/ATR workbench.

Workstation	Lenovo ThinkStation D10
Processor	Xeon X5460 3.16 GHz dual quad-core
RAM	32 GB
HD for applications	146 GB
HD for data	2 TB in RAID 5 setup
Video graphics card	Nvidia FX4600 with 768 MB DDR3 memory
Permanent storage	DVD drive with blue-ray burner
Operating System	Windows XP Professional 64-bit

2.2 Software

The workbench shelters a software framework for supporting and interfacing a series of processing modules aimed at visualizing, creating, manipulating and storing 3D data. The software architecture of the workbench is designed to be modular and reconfigurable. Implementation was done in C/C++ using Microsoft Visual Studio 2005 Professional, compiled under 64-bit configuration.

The workbench features an Operator-Machine Interface (OMI) which allows the user to interact with the different software modules and to view the different data types. The OMI is developed in *Qt* with the tool *Qt Designer*, which facilitates Graphical User Interface (GUI) design from *Qt* components. *Qt*'s *Signals-and-Slots* mechanism is used within the OMI to handle communication between the different windows. *Coin3D* is the 3D graphics API used for 3D visualization, since it is highly efficient in handling large datasets, such as point clouds. *Qt* and *Coin3D* are linked with the *Quarter* widget. *Qt Phonon* multimedia framework is used to play video with the *ffdshow* codec.

The ATD/ATR simulation environments is designed to allow the user to develop algorithms in Matlab®. The Matlab® Compiler™ is used to generate executables with command line parameters, which are then integrated in the workbench. This flexible interfacing solution between the workbench and the ATD/ATR algorithms avoids recompilation of the entire workbench given the addition of a new algorithm.

3. WORKBENCH CAPABILITIES

The following sections briefly describe the designed workbench capabilities in terms of implemented database functionalities, data processing tools and 3D ATD/ATR simulation environments.

3.1 Database Management System

A Database Management System (DBMS) is integrated to the workbench to manage a variety of data sources and formats from different sensors and input files. The DBMS also assists with navigating through multiple datasets collected in field trials or created by workbench modules, and provides a readily accessible data resource for selecting training data and testing data for the ATD/ATR algorithms.

3.1.1 DBMS components

The DBMS is essentially comprised of three components: the Controller, the Database and the File Manager. The Controller component provides an interface between the Database and the Database OMI. It passes SQL queries to the Database and receives the results. It also initiates file transfers to and from a File Storage System through the File Manager component. The Database component provides an interface to a PostgreSQL database from the Controller component. It is comprised of the PostgreSQL 8.3.7 database and the *libpq* C library. The File Manager component provides an interface to the DBMS File Storage System for the Controller component. It uses Windows XP calls to perform file management operations and maintains the DBMS's internal file organization.

3.1.2 Database structure

A flexible database structure is designed, based on defining relationships between generalized entities. As an example, Fig. 2 illustrates the entity and relationship structure for 2D/3D source data. The arrowheads and arrowtails indicate a *belongs-to* or a *has-a* relationship respectively, while the numerics indicated the number of permitted relationships. For instance, each Point Cloud entity can belong to only one Library entity, but a Library can have up to N Point Clouds. Library and Mission entities are top-level organizational categories and are subject to an exclusive OR condition. This implies that a Point Cloud can belong to either a Library or a Mission, but not both.

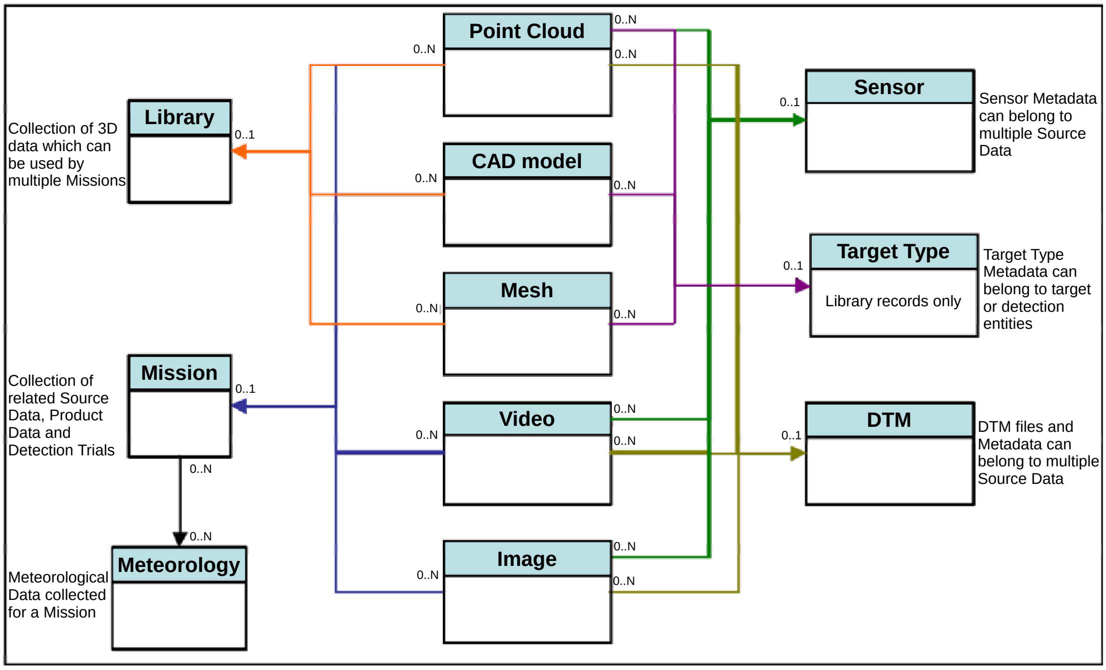

Figure 2. Database entity and relationship structure for 2D/3D Source Data.

Additional DBMS structures, not shown here, have also been designed for 3D data derived from workbench modules, for ATD/ATR algorithm results and for performance-assessment data.

3.2 Data Processing Tools

When data requires manipulation prior to the study of ATD/ATR, data processing tools from the Processing Module in Fig. 1 may be used. These tools, which will now be briefly described, include range data processing, surface mesh generation, shape-from-motion (SfM) extraction and texture mapping.

3.2.1 Point-cloud registration

This tool registers two point clouds taken from different viewpoints. Registration may be performed automatically for high-resolution point clouds with close viewpoints. Otherwise, a semi-automatic approach allows the operator to provide coarse alignment prior to refinement using automatic registration. The *VRMesh* library is used for both semi-automatic and automatic registration and exploits a technique derived from the Iterative Closest Point (ICP) algorithm.[7]

3.2.2 Point-cloud segmentation

Two types of point-cloud segmentation are supported with this in-house tool. The first is a 3D box or sphere specified by the user and the second is automatic and semi-automatic ground segmentation. If ground points are predominant in the scene, automatic ground segmentation is performed by applying the Random Sample Consensus (RANSAC) algorithm.[8] For semi-automatic ground segmentation, the user can select three or more points on the ground to be fed to a least-squares plane fitting algorithm. Inliers within a given threshold of this plane are then associated with the ground plane. Once the ground plane is established, points above a user-specified altitude may also be segmented. This allows the user to discard data high above ground-level which are most likely not associated to a target, such as tree tops, power lines or high buildings.

3.2.3 Point-cloud meshing

A meshing tool allows the user to convert a point cloud to a triangular mesh with configurable parameters. This tool can be used for compression, decimation, denoising, rendering or smoothing. The *VRMesh* library is used for meshing, based on a proprietary algorithm derived from the Marching Cubes algorithm.[9]

3.2.4 Ground truthing

This in-house tool allows the user to manually annotate each point cloud in order to establish ground truth information for test data. The operator can create a bounding box around each target and then enter the ground truth data, such as vehicle type, target coordinates and other descriptions, which is added to the database. This procedure is repeated for each target in the scene.

This information is then used when performing ATD/ATR performance evaluation. During ATD/ATR evaluation, detection and recognition results are compared to the ground truth data and performance is rated by plotting various metrics.

3.2.5 Motion stereo

Significant efforts were made to develop an in-house Shape-from-Motion (SfM) tool. This module is designed to extract a realistic 3D representation of a scene or a target from a stream of images, acquired either by a video camera or a digital frame camera. As motion stereo is an active research topic in the field of computer vision, this SfM module is semi-automatic and still under development.

The SfM module performs image registration for 3D extraction from stabilized or unstabilized image sequences. Additionally, texture-mapping capabilities are also implemented for 3D meshes (created from SfM point-cloud data) to produce photo-realistic 3D models.

Fig. 3 illustrates the high-level flowchart of the Shape-from-Motion module. Video or image stream can be handled provided that navigation data (GPS/INS metadata) and camera calibration parameters are available.

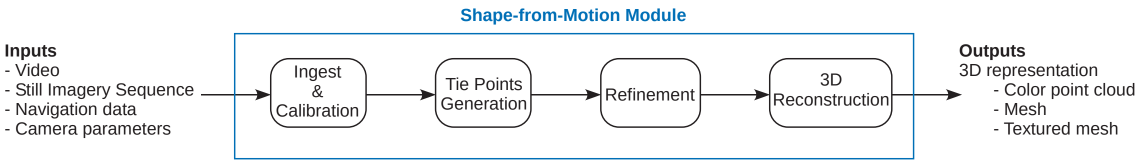

Figure 3. High-level flowchart of the Shape-from-Motion module.

The user first selects an image sequence subset on which to perform SfM. For image series, the user can define a subimage Region of Interest (ROI) from the image set. For videos, the user can crop a segment of the original video. Tie points are then generated between individual video frames or between still images. SIFT features[10] are used to create tie points between still images and *SynthEyes* is used for tie-point generation and feature tracking in video frames.

Refinement is then performed for both video and still imagery. N-fold 2D tie points and coarse camera poses (based on GPS/INS metadata) are used for bundle adjustment to refine the camera poses and tie points simultaneously. Accurate tie points are critical for the refinement process and must have an acceptable distribution over all the images in order to produce quality refined geometries after bundle adjustment.

3D reconstruction then processes the input frames with the refined camera poses to generate a 3D point cloud. A pair-wise approach is used where image pairs suitable for 3D reconstruction are selected and correlation-based dense-stereo matching is used to extract a 3D point cloud for each pair. The 3D point clouds of each valid image pair are then merged together to produce an overall 3D point cloud. Moreover, when color images are used, an RGB value can be assigned to each point, thus producing colored point clouds.

Optionally, the resulting point cloud can be converted to a triangular mesh. A texture mapping module then applies the texture images to the mesh to produce a photo-realistic 3D model. As each triangle in the mesh can be observed by multiple frames, two criteria for texture mapping are implemented: the first is to use the minimal number of texture images and the second is to select the best image for each triangle. The first criterion is generally preferred, since it ensures that only images that cover a large number of triangles are selected. The resulting 3D model thus have fewer visible seam lines and are faster to load and to visualize.

3.3 3D ATD/ATR Simulation Environments

At the core of the workbench are simulation environments tailored for the study of 3D ATD and 3D ATR. These environments include a synthetic range image generation tool, 3D ATD/ATR algorithms and performance metrics for ATR.

3.3.1 Synthetic point-cloud and range image generation

This in-house tool enables the user to render synthetic data for characterizing ATD/ATR algorithms. Rendering is performed by simulating a laser scanner using a ray tracing technique[11] and by sampling a synthetic scene created with CAD models.

This point-cloud generation tool can thereby sample a synthetic scene from any user-defined viewpoint. It also supports loading of multiple CAD models to emulate target occlusion by various foreground objects. When sampling a synthetic scene, user-defined scanning parameters control the sampling density on target, as well as the additive noise on the range and on mirror angles.

Additionally, this tool also uses ray tracing to produce 2D images. Batch processing produces 2D views from multiple predefined viewpoints around the target. This functionality will prove useful for generating target signatures from different viewpoints for multi-view ATR algorithms.

3.3.2 Algorithm prototyping

The main purpose of the workbench is to assess the performance of 3D ATD/ATR algorithms. The workbench is designed to support easy integration of new algorithms without having to recompile the workbench. Algorithms are first prototyped in Matlab® for maximum flexibility and the Matlab® Compiler™ is then used to generate executables with command line parameters. New algorithms and their argument list are added to a configuration file and the OMI automatically generates an interface for that algorithm featuring definable parameters.

An extensive literature review was done in the field of 3D free-form object detection and recognition. For 3D ATR, this survey focused mostly on: 1) silhouette-based approaches, which are view-based; 2) geometry-based approaches, which are model-based and exploit the properties of a point cloud, and; 3) feature-based approaches, which are also model-based but exploit 3D shape descriptors derived from a point cloud. This work has led to a short list of candidate algorithms most suitable for airborne ISR applications. As a starting point, three algorithms have been selected and are currently being integrated in the workbench. The first is a 3D ATD algorithm for analyzing forested scenes,[12] while the others are 3D ATR algorithms derived from tensor-correspondences[13] and rectangle estimation.[14] Additional algorithms found in the literature are expected to be integrated in the workbench and new in-house algorithms will also be added.

3.3.3 ATR performance metrics

Once ATR algorithms are implemented, performance metrics will be required to quantify accuracy and efficiency and to highlight strengths and weaknesses. Performance assessments will first be evaluated for each individual algorithms. Metrics, such as ROC curves and confusion metrics, will characterize the sensitivity as a function of discrimination thresholds and provide statistical measures on the quality of the ATR process. Performance assessments will also be performed between algorithms. Metrics, such as histograms, will compare various attributes such as true-positive rates, false-positive rates and processing time. A thorough and comprehensive performance evaluation will require running various ATD and ATR algorithms using a range of algorithmic parameters across many datasets. To facilitate this, the workbench supports batch mode execution of ATD and ATR algorithms.

4. DATA COLLECTION TRIALS

Approximately 70 GB of data has been collected during two field trials at Valcartier Garrison and at DRDC Valcartier in Québec City, Canada. In February 2009, a first data collection campaign focused on scanning military and civilian vehicles to produce 3D reference models. In July 2009, airborne field data was collected over designated areas where targets were dispatched according to various cooperation scenarios. The objective of both these trials was to populate the database in anticipation of a broad 3D ATD/ATR study.

4.1 Ground Scans of Vehicles

In the first field trial, civilian and military vehicles were scanned to produce high-resolution 3D models. Data acquisition was performed using a tripod-mounted Leica ScanStation 2. This survey-grade scanner offers a selectable field-of-view with a boresighted RGB camera. Each vehicle was scanned repeatedly from different perspectives and scans were finely registered to produce a 3D model, as illustrated in Fig. 4. Circular and spherical targets were placed on each vehicle to facilitate registration. An RGB image of each perspective was taken in order to produce colored 3D point clouds. For each perspective, a 3 mm $\times$ 3 mm sampling grid was set at the farthest visible edge of the vehicle. The resulting 3D models have resolutions down to the sub-millimeter range.

Figure 4. 3D model of a military vehicle in colored point-cloud form, obtained from 6 scans with different perspectives (color image available online).

A total of 26 vehicles were scanned (15 from Canadian Forces and 11 civilian), each of which is depicted in Fig. 5. To produce accurate and complete 3D models, each vehicle required to be scanned from 4 to 11 different perspectives, depending on vehicle dimensions and self-occlusion. The resulting 3D models consist of high-resolution colored point clouds with 600,000 to 5,000,000 points.

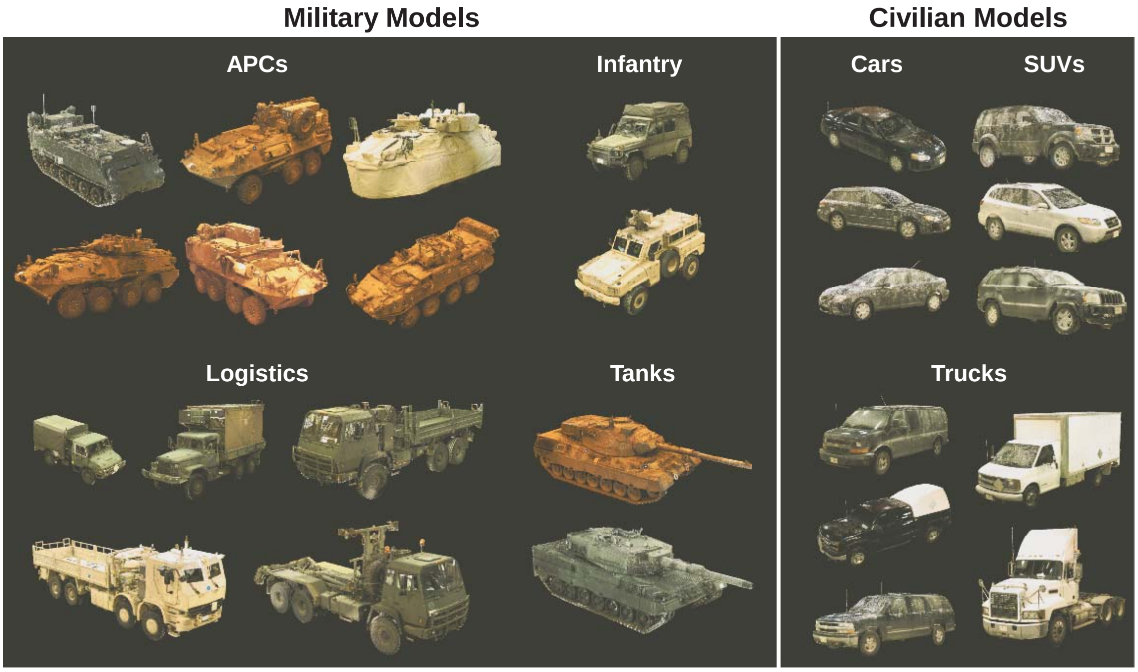

Figure 5. Database of 26 scanned vehicles, resulting in high-resolution 3D models for 15 Canadian Forces vehicles and for 11 civilian vehicles (color image available online).

4.2 Airborne Data Collection

In the second field trial, a heliborne data collection campaign was conducted. The payload consisted of a ladar, a video camera and a digital camera. Data collection thus consisted of 3D ladar imaging and still imagery/video for 3D shape extraction by motion stereo. Ladar data was acquired with a full-waveform digitizing Riegl LMS-Q560. A boresighted Canon EOS-1Ds digital camera with a 64 deg FOV, 4064x2704 resolution and 0.16 Hz frame rate, was used to acquire still imagery. Also, a boresighted Pixelink PL-B742F video camera with a 37.7 deg FOV, 1280x1024 resolution and 5 Hz frame rate, was used to capture video. The still imagery was acquired in a grid pattern at 200 m AGL with 80% overlap and 75% sidelap. Video was also acquired in a grid pattern at 200 m AGL, but with 50% overlap. Ladar data was acquired simultaneously with either still imagery or video during flights. The average point cloud density varies from 100 points/m^2 to 1250 points/m^2 with an accuracy of 9 cm RMS.

For calibration purposes, a ground control point was setup on-site by static GPS during data collection and three receivers were in operation during the flights. Two calibration sites were also measured with a total station for ladar and imagery calibration. Some ground control points were also established around hangars with a GPS RTK and a kinematic survey was conducted to control ladar accuracy.

Within the five sectors flown, dozens of civilian and military targets were deployed prior to fly-by. In each case, scenarios were implemented, ranging from simple cooperative targets (e.g. open parking lots) to highly uncooperative targets (e.g. concealed targets under trees and camouflage nets). The sectors scanned included forested areas, where occlusion is most likely caused by dense vegetation, and urban areas, where occlusion is most likely caused by man-made objects, such as buildings.

For example, Fig. 6 depicts a tile of 3D ladar imagery of an urban area. Two cooperative targets are clearly shown parked near buildings. Although automation of the ATD/ATR processes remains challenging, these target-cooperation scenarios are considered simple. Complex target-cooperation scenarios are presented in Fig. 7. This sample of 100 m $\times$ 100 m 3D ladar imagery features two concealed targets in a forested area. A first vehicle (left) was positioned in dense vegetation with no overhead obstruction. A second vehicle (right) was parked head-first in dense vegetation and a camouflage net was deployed over-top.

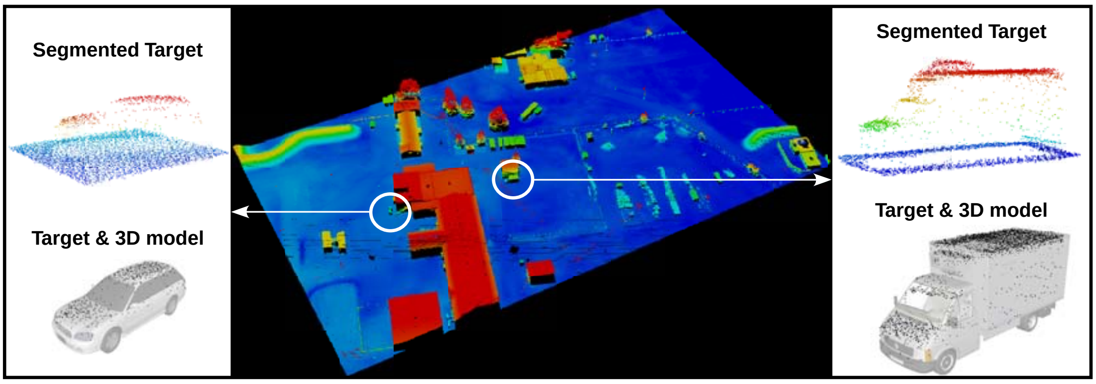

Figure 6. Sample airborne ladar imagery of an urban scene featuring two cooperative targets. The elevation above ground is color-coded (color image available online). The truck (on the right) featured a ventilation unit on top that is not depicted on the 3D model. The car (on the left) did not remain parked at the same location during all fly-bys, which explains the ground points beneath the target. CAD models presented here were downloaded from www.3dcadbrowser.com.

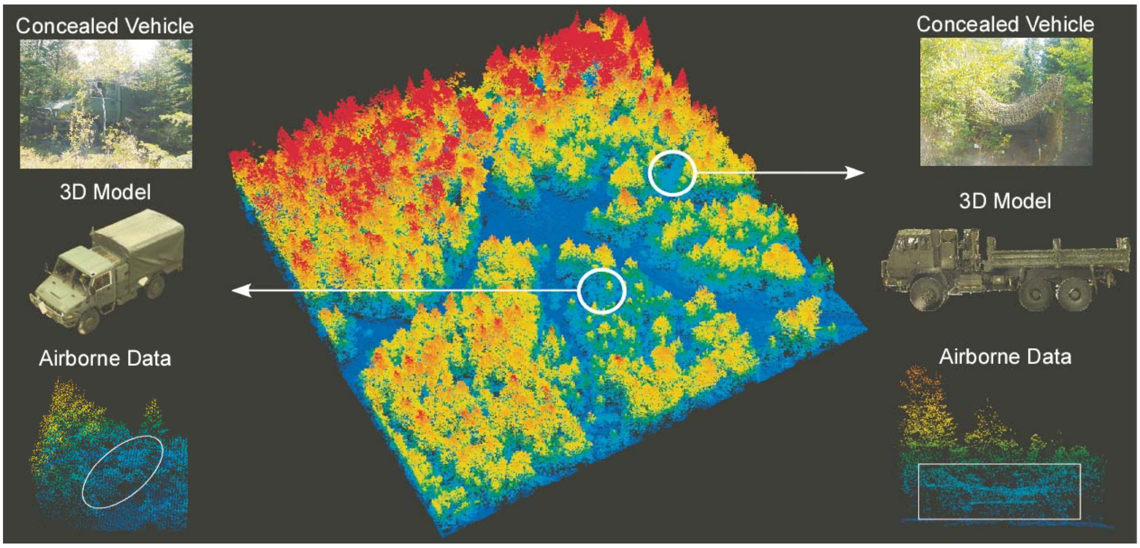

Figure 7. Sample airborne ladar imagery of a forested scene featuring two concealed targets. The elevation above ground is color-coded (color image available online).

5. PRELIMINARY RESULTS

Since 3D ATD/ATR simulation environments are still under development, the preliminary results presented in this section are limited to the 3D shape extraction capabilities from motion stereo.

5.1 3D Reconstruction by Motion Stereo

3D extraction has been mostly performed from streams of high-resolution still imagery acquired during airborne field trials. Preliminary results presented in Fig. 8 show how a common ROI on an image pair is reconstructed into a triangular 3D mesh without mapped texture. This image pair produces over 800,000 3D points and the mesh consists of around 60,000 triangles. Similarly, Fig. 9 presents 3D textured meshes which highlight an area under construction and a tent-like building.

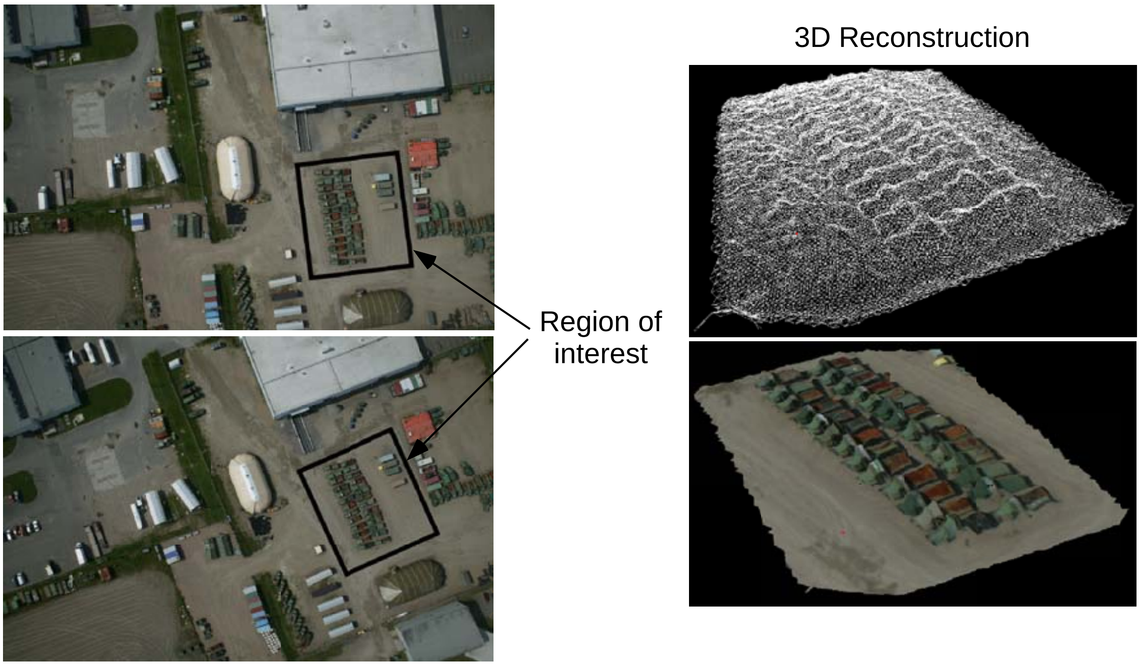

Figure 8. On the left, two high-resolution images, automatically selected from an image sequence, show the user-defined ROI on which SfM processing was applied (color image available online). On the right, the resulting 3D representation obtained from the image-pair, presented as a triangular mesh (top-right) and a textured mesh (bottom-right).

Figure 9. Textured meshes obtained from motion stereo (color image available online). Left: 3D reconstruction of a scene featuring an area under construction. Right: 3D reconstruction of a scene featuring a tent-like building.

6. FUTURE WORK

Upcoming work will focus on evaluating 3D sensing technologies and 3D ATD/ATR algorithms for ISR applications. The workbench will be exploited as an investigation tool for comparative performance assessment. New datasets collected from previous trials with different 3D sensors are expected to be integrated in the database for comparative study. Also, additional 3D ATD/ATR algorithms will be implemented, stemming from a literature survey of published work. New algorithms will also be prototyped, tailored to specific sensing technologies and to the specific requirements of ISR applications. A broad study will be conducted to investigate impacts related to 3D target representation, such as point cloud density of 3D models, occlusion, points on target, range uncertainty, as well as impacts related to sensing requirements such as signal-to-noise ratio, sensor type and sensor fusion. Other work will focus on exploiting a priori mission knowledge, such as DTMs, digital maps, satellite imagery and meteorology data.

7. CONCLUSION

The current status of the DRDC 3D ATD/ATR workbench has been described. The workbench consists of a database, a toolbox for data processing, including motion stereo capabilities, and 3D ATD/ATR simulation environments. The main objective of the workbench is to enable exploration, development, and optimization of advanced ATD/ATR capabilities for airborne ISR applications. This tool will be exploited in a broad study to investigate promising 3D sensing technologies and 3D data exploitation techniques. The ultimate motivation of this work is to progress towards realizing an automatic 3D ATD/ATR data processing pipeline. This capability may contribute to increase Canadian Forces survivability through robust situational awareness, accurate target identification and rapid response to tactical threats.

ACKNOWLEDGMENTS

The authors would like to thank the military personnel from the 12e Régiment blindé du Canada, the 5e Bataillon des services du Canada and the 430e Escadron tactique d'hélicoptères, stationed at Valcartier Garrison, for their involvement in field trials. The authors would also like to thank Geolocation Inc. for data collection, the DRDC technicians for their support during field trials and the MDA A3DS project team for their contribution.

REFERENCES

[1] Armbruster, W., "Comparison of deterministic and probabilistic model matching techniques for laser radar target recognition," *Proc. SPIE* **5807**, 233–240 (2005).

[2] Andersson, P., "Long-range three-dimensional imaging using range-gated laser radar images," *Opt. Eng.* **45**(3), 1–10 (2006).

[3] Li, X. and Guskov, I., "3D object recognition from range images using pyramid matching," *IEEE ICCV* , 1–6 (2007).

[4] Jelalian, A. V., [*Laser Radar Systems*], Artech House, Norwood, MA, 292 pages (1992).

[5] Sobel, E., Douglas, J., and Ettinger, G., "3D ladar ATR based on recognition by parts," *Proc. SPIE* **5094**, 29–40 (2003).

[6] Vasile, A. and Marino, R., "Pose-Independent Automatic Target Detection and Recognition Using 3D Laser Radar Imagery," *Lincoln Lab. J.* **15**(1), 61–78 (2005).

[7] Besl, P. and McKay, N., "A method for registration of 3-D shapes," *IEEE T-PAMI* **14**(2), 239–256 (1992).

[8] Fischler, M. and Bolles, R., "Random sample consensus: A paradigm for model fitting with applications to image analysis and automated cartography," *Comm. ACM* **24**(6), 381–395 (1981).

[9] Lorensen, W. and Cline, H., "Marching cubes: A high resolution 3D surface construction algorithm," *Proc. CGIT* **21**(4), 163–169 (1987).

[10] Lowe, D., "Distinctive image features from scale-invariant keypoints," *Int. J. Comput. Vis.* **60**(2), 91–110 (2004).

[11] Whitted, T., "An improved illumination model for shaded display," *Comm. ACM* **23**(6), 343–349 (1980).

[12] Grönwall, C., Chevalier, T., Tolt, G., and Andersson, P., "An approach to target detection in forested scenes," *Proc. SPIE* **6950**(69500S), 1–12 (2008).

[13] Mian, A., Bennamoun, M., and Owens, R., "Three-dimensional model-based object recognition and segmentation in cluttered scenes," *IEEE T-PAMI* **28**(10), 1584–1601 (2006).

[14] Grönwall, C., Gustafsson, F., and Millnert, M., "Ground target recognition using rectangle estimation," *IEEE T-IP* **15**(11), 3400–3408 (2006).